THE ROYAL SOCIETY

Received 19 April 2002
Accepted 5 June 2002

Interaction between seasonal density-dependence structures and length of the seasons explain the geographical structure of the dynamics of voles in Hokkaido: an example of seasonal forcing

Nils Chr. Stenseth[1]*, Marte O. Kittilsen[1], Dag Ø. Hjermann[1], Hildegunn Viljugrein[1] and Takashi Saitoh[2]

[1] *Division of Zoology, Department of Biology, University of Oslo, PO Box 1050, Blindern, N-0316 Oslo, Norway*
[2] *Field Science Centre, Hokkaido University, North 11, West 10, Sapporo 060-0811, Japan*

The grey-sided vole (*Clethrionomys rufocanus*) is distributed over the entire island of Hokkaido, Japan, across which it exhibits multi-annual density cycles in only parts of the island (the north-eastern part); in the remaining part of the island, only seasonal density changes occur. Using annual sampling of 189 grey-sided vole populations, we deduced the geographical structure in their second-order density dependence. Building upon our earlier suggestion, we deduce the seasonal density-dependent structure for these populations. Strong direct and delayed density dependence is found to occur during winter, whereas no density dependence is seen during the summer period. The direct density dependence during winter may be seen as a result of food being limited during that season: the delayed density dependence during the winter is consistent with vole-specialized predators (e.g. the least weasel) responding to vole densities so as to have a negative effect on the net growth rate of voles in the following year. We conclude that the observed geographical structure of the population dynamics may be properly seen as a result of the length of the summer in interaction with the differential seasonal density-dependent structure. Altogether, this indicates that the geographical pattern in multi-annual density dynamics in the grey-sided vole may be a result of seasonal forcing.

Keywords: *Clethrionomys rufocanus*; state-space modelling; geographical gradient; winter food shortages; predation; predator-swamping

1. INTRODUCTION

Rodent species exhibiting periodic multi-annual density cycles typically do so only in parts of their distribution range (Hansson 1971; Hansson & Henttonen 1985, 1988, 1998; Stenseth 1999). For example, populations of the grey-sided vole, *Clethrionomys rufocanus* (named by Sundevall 1846) in northern and eastern parts of Hokkaido, Japan, exhibit multi-annual periodic density fluctuations superimposed upon a seasonal dynamic pattern, with population growth during summer and decline during winter (Saitoh 1987; Stenseth *et al.* 1996; Bjørnstad *et al.* 1998, 1999; Saitoh *et al.* 1998, 1999, 2002). In the southern and western parts of Hokkaido, populations of the species exhibit only seasonal dynamics.

Several mechanisms have been suggested to explain the geographical variability in dynamics of small rodents: differences in the predator guild (e.g. Hansson & Henttonen 1988; Hanski *et al.* 1991; Bjørnstad *et al.* 1995; Turchin & Hanski 1997; Korpimäki *et al.* 2002), primary productivity (e.g. Jedrzejewski & Jedrzejewska 1996) and/or in climatic conditions (such as seasonality and extent of snow-cover (e.g. Hansson & Henttonen 1985; Hansson 1987; Bjørnstad *et al.* 1998; Hansen *et al.* 1999)). Expanding on the latter idea, Åström *et al.* (1996) (see also Kot & Schaffer 1984; Rinaldi *et al.* 1993; Grenfell & Finkenstädt 1998; Lindström *et al.* 2001) suggested that different density-dependent structures within each of the seasons might represent a mechanism leading to multi-annual periodic cycles only in parts of a species' range of distribution. The proposition that the relative length of the seasons determines whether a population is cyclic or not is referred to as 'seasonal forcing'.

In this paper, we demonstrate that the estimated annual density dependencies exhibit a clear geographical structure, and that this geographical structure might be a result of the relative length of the summer season at different locations within Hokkaido. On this basis, we empirically strengthen the conclusion of Stenseth *et al.* (1998) that shortening the summer length will change the annual dynamics from no multi-annual density cycles to multi-annual density cycles. Here, we expand and improve on the earlier analysis reported by Stenseth *et al.* (1998) in four respects.

(i) We use estimates for the direct and delayed density dependencies obtained through a statistical model incorporating sampling variance. For this purpose, we explicitly model the sampling process by adopting a state-space modelling approach (cf. Fahrmeir & Tutz 1994) and by so doing reducing biases inherent in the more classical autoregressive approach (see Ludwig & Walters 1981; Reddingius & den Boer 1989; Rothery 1998; Shenk *et al.* 1998).

---

* Author for correspondence (n.c.stenseth@bio.uio.no).

DOI 10.1098/rspb.2002.2099

(ii) We document the geographical structure of the pattern of density-dependent dynamics, using geographical coordinates as predictors of the density-dependent coefficients in the autoregressive model.
(iii) We use a seasonal decomposition of the annual dynamics being improved compared with that used by Stenseth *et al.* (1998). By so doing, the estimated direct density dependencies during summer and winter are directly comparable.
(iv) We deduce (empirically) an index for the length of the summer season being a descriptor of the geographical structure of the annual direct and delayed density dependencies. This quantity (τ) is then used as an index for decomposing the seasonal structure of the annual density dependencies.

Although our focus on the seasonal density-dependent structure is similar, the approach taken in this paper is different from that of Hansen *et al.* (1999), Merritt *et al.* (2001) and Stenseth *et al.* (2002), who used data on both spring and autumn densities to assess the seasonal density-dependent structure of the same species. Whereas Hansen *et al.* (1999) and Stenseth *et al.* (2002) made the tacit assumption of the spring and autumn sampling coinciding with the termination of the winter and the summer seasons, we do in this study let the annual density-dependent structure 'tell us' how the year is most appropriately to be divided into two phases (which we will call 'seasons' and refer to as 'summer' and 'winter').

2. THE STUDY AREA AND THE VOLE DATA

Hokkaido is the northernmost island (41°24′ –45°31′ N, 139°46′ –145°49′ E) of Japan and covers an area of 78 073 km^2. This island neighbours the Asian continent and is surrounded by the Sea of Okhotsk, the Pacific and the Sea of Japan (figure 1). A southern warm current prevails in the Sea of Japan along the western shore of Hokkaido, whereas a northern cold current prevails in the Pacific along the northern and eastern shores. Mountain ridges run north–south through the middle of the island and in the southwestern part there is another mountain ridge. Except for the southwestern peninsula harbouring temperate deciduous forests, most of the natural forests in Hokkaido are characterized by a transition type of forest between the temperate and the subarctic zones (Tatewaki 1958). The dominant tree genera are *Abies*, *Acer*, *Betula*, *Picea* and *Quercus*.

Hokkaido represents the easternmost part of the grey-sided voles' distribution, ranging from its westernmost edge in Fennoscandia (see Kaneko *et al.* 1998). The grey-sided vole (*C. rufocanus*) represents a pest on plantations of larch (*Larix leptolepis*) and todo-fir (*Abies sachalinensis*). Since 1954, the Forestry Agency of the Japanese Government has carried out censuses of vole populations for management purposes in forests all over Hokkaido. The forests managed by the Forestry Agency cover 28 400 km^2 (21 500 km^2 of natural forests and 6900 km^2 of planted forests—1992 figures). These forests were, in 1992, managed by 76 district offices, which were further divided into several ranger offices, giving a total of 433 ranger offices.

Rodent censuses were carried out by the individual ranger office, which also represented our basic unit of analysis; personnel at the ranger offices were regularly trained for performing the censuses, including species identification (see Kaneko *et al.* 1998). The censuses were carried out three times a year (spring (May or June), summer (July or August) and autumn (September or October)) on a 0.5 ha (50 m × 100 m) plot, where 50 snap traps were set at 10 m intervals for five or three nights. Each ranger office censused two to six separate grids. Census grids were located in fixed pre-selected habitats (planted forest and natural forests neighbouring a plantation, which together constituted a unit). We have, in this paper, omitted data from planted forests in order to exclude the influences of pest control using poisonous baits. The census grids were occasionally relocated within the area of a given ranger office. (For further details, see Bjørnstad *et al.* (1996); Stenseth *et al.* (1996) and Saitoh *et al.* (1997).)

The grey-sided vole is the most common rodent species in Hokkaido (Ota 1958, 1984; see also Stenseth *et al.* 1996). Three other microtine and murine rodent species are recorded as an integral part of the census: *Clethrionomys rutilus* (named by Pallas 1779), *Apodemus speciosus* (named by Temminck 1844) and *A. argenteus* (named by Temminck 1844). In addition, *C. rex* (named by Imaizumi 1971), *A. peninsulae* (named by Thomas 1907) and shrews (*Sorex* spp.) are occasionally caught. *Clethrionomys* is easily distinguished from other rodents. Distinguishing *C. rufocanus* from its congeners may be difficult. However, the abundance of *C. rutilus* and *C. rex* is typically fairly low in Hokkaido (Ota 1984; Saitoh & Nakatsu 1997), minimizing the possible effect of any misclassification.

The summer season is the main reproductive period (breeding usually starts at around snow melt (April/May) and continues until September/October). Winter reproduction is negligible in the grey-sided vole in Hokkaido (Ota 1984; Kaneko *et al.* 1998). However, voles are still active in winter under the snow cover. Their main food item during the winter is the leaves of bamboo grasses (*Sasa* spp.) (Ueda *et al.* 1966), which are quite abundant but nutritionally rather poor. Hokkaido is rich in predators such as snakes, birds and mammals (Henttonen *et al.* 1992); however, their activity under snow cover is rather restricted for most of these species, one exception being the least weasel (*Mustela nivalis*), which is the most important predator under snow cover (e.g. Hansson & Henttonen 1985; Hansson 1987).

In the present paper, we use, following what is typically done (e.g. Stenseth *et al.* 1998), only the autumn data. We used the total number of caught grey-sided voles, together with the corresponding trapping efforts, as our basic data. Trapping effort is defined by multiplying the number of traps by the number of nights and the number of census plots. For example, when three night censuses were carried out at three grids in a ranger office, the trapping efforts by the ranger office at the census was 450 (50 × 3 × 3). Trapping effort in year t is given as T_t.

The studied populations include both multi-annual cyclic (groups 2, 3 and 5; see figure 1) and multi-annual non-cyclic (groups 1, 4, 7, 6 and 8) populations (e.g. Bjørnstad *et al.* 1998). Each site was assigned geographical coordinates (g_{we} and g_{sn}, where g_{we} and g_{sn} are defined as the location in the west–east and the south–north directions, respectively, single coordinate units of which correspond

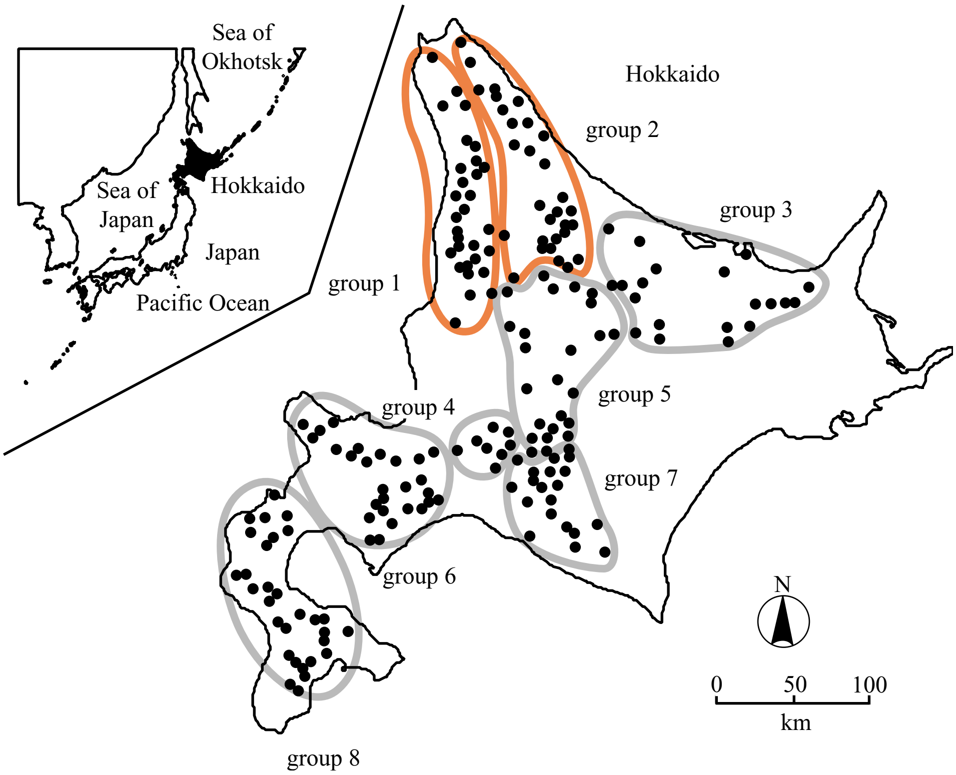

Figure 1. Map of the study area, Hokkaido, being the northern-most island of Japan. The 189 studied populations have been grouped according to topographical characteristics (see Saitoh *et al.* (1998) for details).

to 2 km, and the southeastern part of Hokkaido having the lowest point) and the height above sea level (h, being measured in units such that 1 corresponds to 10 m).

3. METHODS OF ANALYSIS

(a) *The ecological annual model*

We explicitly incorporate sampling variance when estimating the density-dependent structure by adopting a state-space modelling approach (e.g. Fahrmeir & Tutz 1994; Meyer & Millar 1999*a*,*b*; de Valpine & Hastings 2002). Below, we outline the underlying ecological model. The statistical model linking the observations to the ecological variables in this ecological model—this paper's first major improvement over Stenseth *et al.* (1998)—is presented in Appendix A.

Defining α_1 as the direct density dependence and α_2 as the delayed density dependence, a log-linear autoregressive second-order model in which $x_t = \log_e(N_t)$ (where the log-abundances are centred around their respective long-term means and N_t always is assumed to correspond to the non-zero *true* population size at time t) is given by (e.g. Royama 1992; Stenseth 1999):

$$x_t = \alpha_1 x_{t-1} + \alpha_2 x_{t-2} + \varepsilon_t, \qquad (3.1)$$

where ε_t is a normally distributed (time-independent) stochastic quantity describing the process variance with mean equal to zero and fixed variance given by σ^2.

(b) *The geographical structure in the density-dependent dynamics*

In order to uncover the geographical structure of the pattern of density-dependent dynamics, multiple linear regression was performed for the direct (α_1) and delayed (α_2) annual density-dependent coefficients, using the populations' geographical location (g_{we}, g_{sn} and h) as predictors—the second major improvement over Stenseth *et al.* (1998)—starting from the full model $\alpha_i = p_{i,0} + p_{i,1}g_{\mathrm{we}} + p_{i,2}g_{\mathrm{sn}} + p_{i,3}h + p_{i,4}g_{\mathrm{we}}g_{\mathrm{sn}} + p_{i,5}g_{\mathrm{we}}h + p_{i,6}g_{\mathrm{sn}}h + \text{error}$ ($i = 1$ and 2), where $p_{i,j}$ are parameters to be determined by the data. This model assumes that the annual autoregressive coefficients change linearly, (for a given longitude) going eastwards as well as (for a given latitude) going northwards; these linearly increasing rates of change will be different for different longitudes and altitudes as well as for increasing altitude. The best models for α_1 and α_2 were obtained separately through backwards selection (Kleinbaum *et al.* 1988).

(c) *A seasonal model: re-parameterizing the annual model and seasonal forcing*

Stenseth *et al.* (1998) re-parameterized the model given by equation (3.1) by assuming that the summer and winter components of the specific annual net growth rate, R (defined implicitly as $N_t = N_{t-1}R$, where N_t is the population size in the autumn of year t), could be split into two components, one for the summer (R_{summer}, including both reproduction and survival) and another one for the winter (R_{winter}, including only survival); that is: $R = R_{\mathrm{summer}}R_{\mathrm{winter}}$. Let further τ be the length of the summer ($\tau = 1$ corresponds to all summer; $\tau = 0$ corresponds to all winter).

Stenseth *et al.* (1998) assumed spring densities to be mapped onto autumn densities and obtained the following model: $N_t = \text{const} \times N_{t-1} \exp[(-a_{\mathrm{s}1}x_{t-1} - a_{\mathrm{s}2}x_{t-2})\tau] \exp[(-a_{\mathrm{w}1}x_{t-1} - a_{\mathrm{w}2}x_{t-2})(1-\tau)]$, where N_t is the density corresponding to x_t [i.e. $x_t = \log(N_t)$], and 'const' is some scaling parameter of no interest to us in the present context. In this formulation, we then have R_{summer} proportional to

$\exp[(-a_{s1}x_{t-1} - a_{s2}x_{t-2})\tau]$ and R_{winter} proportional to $\exp[(-a_{w1}x_{t-1} - a_{w2}x_{t-2})(1-\tau)]$. A weakness of this re-parameterization is, however, that the winter and summer direct density dependencies (a_{s1} and a_{w1}) are not directly comparable. (The second-order term is assumed to pick up the longer lags due, for example, to specialized predation.)

To avoid this deficiency, we assume some unknown spring density (M_t, with $u_t = \log(M_t)$): this paper's third major improvement over Stenseth *et al.* (1998). In this new formulation, let R_{summer} depend on the density during the previous spring (rather than the previous autumn) and some delayed effect incorporated by the autumn density two years before (just as in the earlier model). With such a formulation of the summer dynamics, the autumn density will now be given as $N_t = C_1 M_t \exp[(-a_{s1}u_t - a_{s2}x_{t-2})\tau]$, where C_1 is a scaling parameter. After some algebra, the new annual model (with seasonal components) can be given as a delay function of autumn densities:

$$N_t = N_{t-1}\, R_{\text{summer}} R_{\text{winter}}, \qquad (3.2a)$$

where

$$R_{\text{summer}} = C_1 \exp[(-a_{s1}\,[\log(C_2) + (1 - a_{w1} + a_{w1}\tau)x_{t-1} - a_{w2}(1-\tau)x_{t-2}] - a_{s2}x_{t-2})\tau] \qquad (3.2b)$$

and

$$R_{\text{winter}} = C_2 \exp[(-a_{w1}x_{t-1} - a_{w2}x_{t-2})(1-\tau)]. \qquad (3.2c)$$

'Seasonal forcing' is interpreted within this model as the length of the season (τ) being a bifurcation parameter determining whether the dynamics is cyclic or non-cyclic. Below, we show that this is in fact the case (see figure 2). Based on equations (3.2*b*) and (3.2*c*), the annual density dependencies in equation (3.1) may be given by the seasonal density-dependent components (direct density dependence during summer (a_{s1}) and during winter (a_{w1}), and delayed density dependence during summer (a_{s2}) and during winter (a_{w2})), and the season length (τ) is found, after some algebra, to be

$$\alpha_1 = 1 - a_{w1} + (-a_{s1} + a_{s1}a_{w1} + a_{w1})\tau - a_{s1}a_{w2}\tau^2, \qquad (3.3)$$

$$\alpha_2 = -a_{w2} + (a_{s1}a_{w1} - a_{s2} + a_{w2})\tau - a_{s1}a_{w1}\tau^2. \qquad (3.4)$$

(The corresponding expressions (3.3) and (3.4) for the re-parameterization originally given by Stenseth *et al.* (1998) are $\alpha_1 = 1 - a_{w1} + (a_{w1} - a_{s1})\tau$ and $\alpha_2 = -a_{w2} + (a_{w2} - a_{s2})\tau$, respectively. The analysis described in Appendix B was performed using this original re-parameterization; the results are presented in electronic Appendix A, tables 4 and 5, available on The Royal Society's Publications Web site.) We used equations (3.3) and (3.4) to estimate the parameters a_{s1}, a_{s2}, a_{w1} and a_{w2} by nonlinear regression through bootstrapping (see Appendix B).

(d) *Deducing an index, τ, for the relative length of the summer season*

The hypotheses regarding seasonal forcing discussed by Stenseth *et al.* (1998) relies on us having a reliable measure of the relative length of the breeding season τ. However, accurate and direct estimates for the relative length of the summer season are difficult to obtain, not least because it varies from year to year. Ideally, we would need some overall measure characterizing the typical season length for any given site.

One possible solution to this problem is further to develop the measure used by Stenseth *et al.* (1998); that is, a model assuming the relative length of the breeding season, τ, to be directly related to the warmth index, WI, given as $\Sigma(\text{Temp} - 5)$, where the sum is taken over the months for which the average monthly temperature, 'Temp', is equal to or above 5 °C (see Kira 1949, 1971). Stenseth *et al.* (1998) demonstrated a close relationship between WI and the geographical scores g_{we} and g_{sn}, and therefore used a τ-index defined on the basis of such geographical scores.

A more empirically (data-based) method of obtaining an assessment of the overall relative length of the seasons (the approach used in this paper) is to ask whether the geographical structure observed in the annual density-dependent structure (see § 4a) can be modelled using the geographical scores to describe the length of the summer season, τ. This is this paper's fourth major improvement over Stenseth *et al.* (1998).

The following relationship is assumed to represent a proxy measure for the relative length of the summer breeding season, τ (motivated by the statistical results relating to the analyses of the geographical structure of the annual density-dependent structure, where g_{we}, g_{sn} and $g_{\text{we}}g_{\text{sn}}$ enter as significant predictors; see table 1):

$$\tau = \exp(F)/[1 + \exp(F)], \qquad (3.5)$$

with

$$F = (b_0 + b_1 g_{\text{we}} + b_2 g_{\text{sn}} + b_3 g_{\text{we}} g_{\text{sn}}), \qquad (3.6)$$

where the parameters b_0, b_1, b_2 and b_3 are to be determined on the basis of data (see Appendix B). This logit-based function will, as required, vary between zero and unity. We expect that the estimated parameters of equation (3.6) yield a large τ for the southwestern part of the island (where the summer breeding season is longest, being heavily influenced by warmer sea currents (e.g. Saitoh *et al.* 1998)). We further expect that τ decreases going northwards and eastwards (towards regions that are increasingly influenced by the colder wind and sea currents (e.g. Saitoh *et al.* 1998)).

4. RESULTS

(a) *The ecological annual model*

Using state-space modelling, 189 pairs of estimates for direct annual density dependence (α_1) and delayed annual density dependence (α_2) have been obtained. (The obtained numerical results are presented in the electronic Appendix, table 3; see also figure 2*a*.) It is worth observing that there is a linear downward 'trend' from the upper-right corner towards the centre of the triangle (the blue line in figure 2*a*). It should also be noticed that if we only use the estimates from groups 1 and 2 (as originally used by Stenseth *et al.* (1996); populations, estimates and lines marked red in figures 1 and 2*a*), there is a counter clockwise 'movement' in the statistical parameter space, just as observed by Stenseth *et al.* (1996); this indicates that the earlier demonstrated counter-clockwise 'movement' is

Table 1. The geographical structure in the annual density dependence.

(The table shows the estimated parameters of the linear regression of (*a*) direct and (*b*) delayed density dependence on g_{we}, g_{sn} and h. (Best models obtained through backwards selection from the full model $\alpha_i = p_{\mathrm{i},0} + p_{\mathrm{i},1}g_{\mathrm{we}} + p_{\mathrm{i},2}g_{\mathrm{sn}} + p_{\mathrm{i},3}h + p_{\mathrm{i},4}g_{\mathrm{we}}g_{\mathrm{sn}} + p_{\mathrm{i},5}g_{\mathrm{we}}h + p_{\mathrm{i},6}g_{\mathrm{sn}}h$.) Confidence intervals (CIs) are based on estimates ± 1.96 s.e.)

parameters	estimate	s.e.	lower 95% CI	upper 95% CI	*t*-value	*p*-value
(*a*) (α_1) (residual error = 0.284; d.f. = 185; $r^2 = 0.271$; $F_{3,185} = 22.94$; $p = 1.14 \times 10^{-12}$; $n = 189$)						
$p_{1,0}$ (intercept)	0.779	0.101	0.580	0.977	7.698	<0.0001
$p_{1,1}$ (g_{we})	−0.005 74	0.001 47	−0.008 61	−0.002 86	−3.906	0.0001
$p_{1,2}$ (g_{sn})	−0.004 04	0.001 08	−0.006 16	−0.001 91	−3.726	0.0003
$p_{1,4}$ ($g_{\mathrm{we}}\,g_{\mathrm{sn}}$)	3.18×10^{-5}	1.31×10^{-5}	6.15×10^{-6}	5.75×10^{-5}	2.431	0.016
(*b*) (α_2) (residual error = 0.265; d.f. = 187; $r^2 = 0.0599$; $F_{1,187} = 11.91$; $p = 0.000\,691$; $n = 189$)						
$p_{2,0}$ (intercept)	0.000 194	0.0455	−0.0889	0.0893	0.004 27	0.997
$p_{2,1}$ (g_{we})	−0.001 63	0.000 471	−0.002 55	−0.000 702	−3.451	0.000 69

Table 2. Estimating the seasonal density dependence from the relationships between the annual density-dependent structure and the relative length of the summer, τ.

(The table shows the estimated parameters for (*a*) direct and (*b*) delayed density dependence for winter (a_{w1}, a_{w2}) and summer (a_{s1}, a_{s2}) growth. Positive values indicated negative density dependence. The standard errors are based on 1000 bootstrap samples and confidence intervals (CIs) are based on estimates ± 1.96 s.e. CIs based on 2.5 and 97.5 percentiles deviated less than 0.02 from the CIs reported here. In the electronic Appendix, table 4, we present the corresponding parameter estimates when it is assumed that spring densities may appropriately be mapped on to autumn densities.)

parameters	estimate	s.e.	lower 95% CI	upper 95% CI	*t*-value	*p*-value
(*a*) (α_1)						
a_{w1}	1.637	0.0365	1.565	1.709	44.795	0.0000
a_{s1}	−0.402	0.227	−0.846	0.0417	1.776	0.0758
(*b*) (α_2)						
a_{w2}	0.351	0.100	0.154	0.547	3.501	0.0005
a_{s2}	−0.166	0.135	−0.430	0.0988	1.228	0.220

only seen in the very northern part of the island and is overshadowed by the downward trend when all sites are used. In view of the much larger dataset used in the present paper, we are convinced that the linear 'trend' in the parameter space seems the more appropriate description of the dynamics on the island.

(b) *The geographical structure in the density-dependent dynamics*

Regressing the direct (α_1) and delayed (α_2) density dependencies on the geographical coordinates, it is seen that two of the three geographical location parameters (the position along the west–east axis, g_{we}, and the position along the south–north axis, g_{sn}) had significant effect on α_1, while only the position along the west–east axis (g_{we}) is a significant predictor of α_2 (see table 1). An interaction between the effects of g_{we} and g_{sn} is observed in the model for α_1. Applying the Akaike's Information Criterion (AIC) (see Burnham & Anderson 1998) instead of the backwards selection results in retention of both g_{sn} and the interaction between g_{we} and g_{sn} in the best model for α_2, but none of these models is profoundly different from the others.

Using the α_1 and α_2 as dependent variables and the geographical location as independent variables (according to the models summarized in table 1), we may predict the 'movement' in the (α_1,α_2) parameter space. This is depicted in figure 2*b*. As can be seen, the process of seasonal forcing emerges: as we move from the southwestern part of the island with long summers towards the northeastern part of the island with short summers, the dynamics changes directionally from non-cyclic to cyclic (multi-annual) dynamics.

(c) *The index, τ, for the relative length of the summer season*

The optimization for finding the best estimates for the parameters (b_0, b_1, b_2 and b_3) of the model predicting the relative length of the seasons, τ (i.e. equations (3.5) and (3.6)), is given in figure 4. Notice that the altitude, h, does not enter into the best linear regression models as given in table 1. This result justifies that we use only the geographical coordinates g_{we} and g_{sn} in the model for τ. With optimal parameter values, equation (3.6) reads $F = 0.998 - 0.011 - g_{\mathrm{we}} - 0.0059 - g_{\mathrm{sn}} + 4.5 \times 10^{-5} \times g_{\mathrm{we}}g_{\mathrm{sn}}$. A graph of the resulting relative season length, τ across geographical space is presented in figure 5. The corresponding predicted trajectory in the (α_1, α_2) parameter space is depicted in figure 2*c*. Again, the seasonal forcing is apparent: decreasing the length of the summer season (τ) changes the dynamics from multi-annual stable to multi-annual cyclic populations. Notice, however, that the lines in figure 2*b* are longer than the lines in figure 2*c*, although both are supposed to model the transition from the southwestern part of Hokkaido to the northeastern part of the island. This is likely to be due to some of the

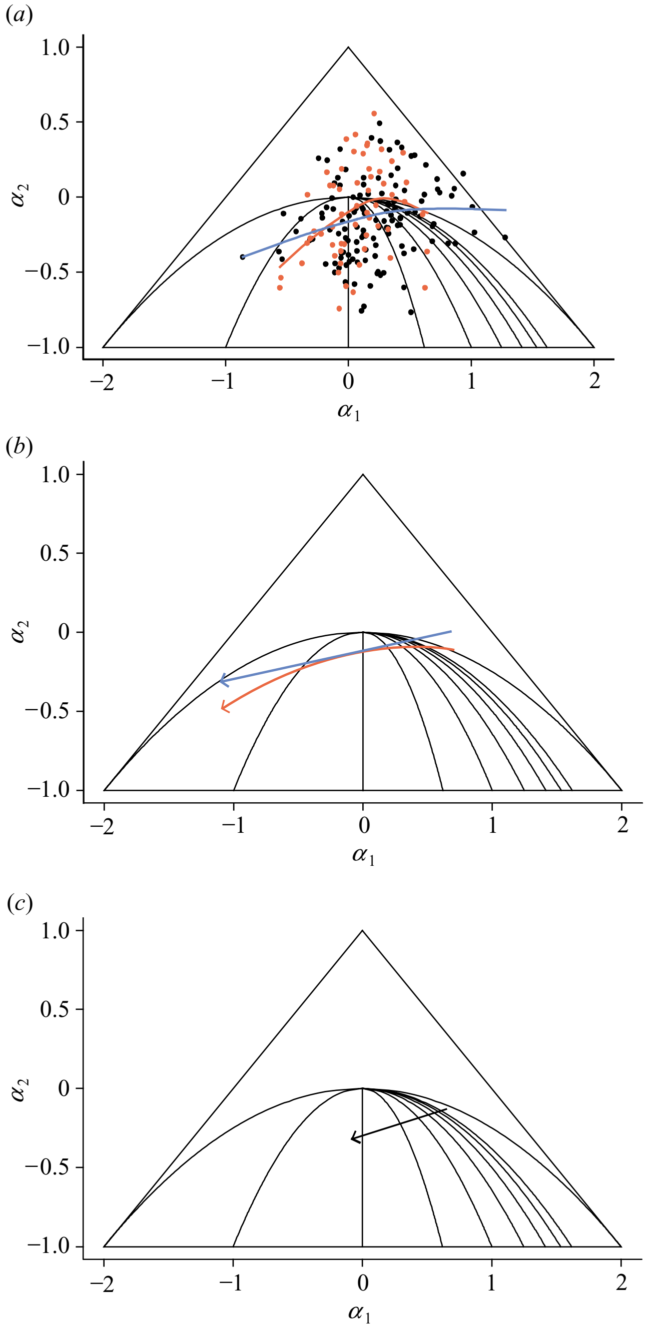

Figure 2. (*a*) The estimated direct (α_1) and delayed (α_2) annual density dependencies (see equation (3.1)) for all 189 populations. Two cubic smoothing splines (d.f. = 3) have been fitted: a blue line for all data and a red line for data from groups 1 and 2 (corresponding data-points are coloured red). (*b*) The movement within the (α_1, α_2) parameter space, along a straight line from the southwest ($g_{\mathrm{we}} = 0$, $g_{\mathrm{sn}} = 24.7$) to the northeast ($g_{\mathrm{we}} = 200$, $g_{\mathrm{sn}} = 179.1$) using the statistically derived model given in table 1. (The α_1 and α_2 density dependencies are as predicted from the statistical analysis using the predictors g_{sn} and g_{we} in models obtained by backwards selection (blue line) or using AIC (red line)). (*c*) The corresponding movement within the same parameter space using the τ-model (see table 2). The contour lines under the parabola within the triangles indicate the period length of the cycle corresponding to the autoregressive parameters; the period increases as going from left to right in the figure.

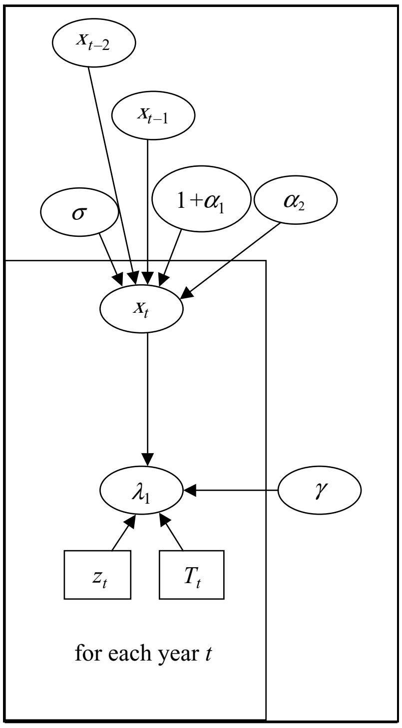

Figure 3. Graphical representation of the annual model (equation (3.1)). The true population abundances are linked to the observations through an observation model (equations (A 1)–(A 3)). The arrows represent prior conditional dependence (stochastic relationship) between nodes (i.e. data observations or unknown parameters in the model). Observed nodes are represented by square boxes and unknown quantities by ellipses. Any node with an arrow emanating from it pointing to some particular node v is referred to as 'parent' of v. There is one 'sheet' for each year t. Quantities without the index t is common for all years.

variance having been accounted for by the τ-model for the length of the summer season (see Appendix B).

(d) *The seasonal model: decomposing the annual density-dependent structure*

The seasonal density parameters are shown in table 2. As can be seen, there is a significant direct density dependence during the winter ($-a_{\mathrm{w1}} = -1.64$; CI: -1.71, -1.57). During summer, there seems to be a somewhat uncertain positive density dependence ($-a_{\mathrm{s1}} = 0.4$; CI: -0.04, 0.85); however, it is clearly weaker than that during the winter season. There is a weak, but statistically significant delayed density-dependent component during the winter ($-a_{\mathrm{w2}} = -0.35$; CI: -0.55, -0.15) but not during summer ($-a_{\mathrm{s2}} = 0.17$; CI: -0.10, 0.43). The simplifying assumption (made by Stenseth *et al.* (1996)) that spring densities are mapped onto autumn densities results in similar conclusions, except that summer growth is not found to be directly density-dependent, but strong and significantly positively delayed density-dependent, the latter of which is most probably an artefact of the simplifying assumption made by Stenseth *et al.* (1998) (see electronic Appendix A, tables 4 and 5).

5. DISCUSSION

In this study, we have demonstrated that the relative length of the seasons is a key factor in determining the

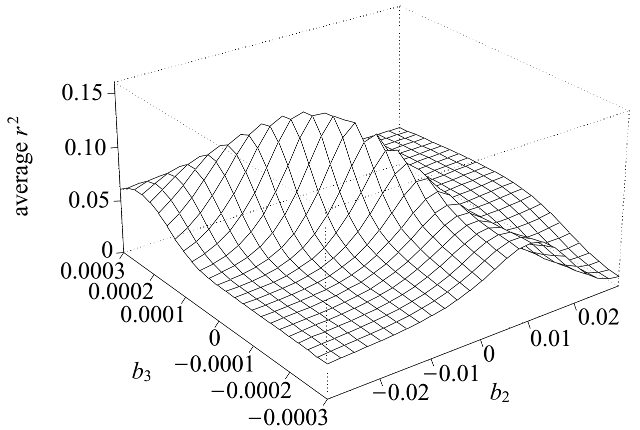

Figure 4. The value of the optimization criterion (vertical axis) for different values of b_2 and b_3. For each point in (b_2–b_3) parameter space, the values of a_{s1}, a_{s2}, a_{w1} and a_{w2} (equations (3.3) and (3.4)) have been found by nonlinear regression. The optimization criterion is the average of the two r^2 values.

geographical density-dependent structure, as well as a key factor in determining whether a population is cyclic or not (i.e. seasonal forcing). By doing so, we have demonstrated that the multi-annual density cycles seen in the grey-sided vole in Hokkaido may be regarded as an example of seasonal forcing (cf. Åström *et al.* 1996; Stenseth *et al.* 1998). Specifically, we have demonstrated that, for the found seasonal density-dependent structure, shortening the length of the summer is sufficient to generate cycles (when starting with a non-cyclic population).

Our results indicate that there is strong direct as well as delayed density dependence during winter. The direct density dependence deduced for the winter period may be seen as a result of depletion of the winter food supply. The delayed density dependence observed for the winter may further be seen as a direct result of specialized vole predators, such as the least weasel: the higher the vole density is during the winter two years earlier, the more the least weasel will be able to build up its own populations, which subsequently will result in a delayed effect two years later (e.g. Hanski *et al.* 1991).

The interpretation of the positive direct density dependence deduced for the summer period is slightly uncertain. This may, however, be a result of predator swamping (e.g. Ims 1990*a*,*b*): given high spring densities of voles, predators may not be able to respond sufficiently fast to have an impact on the vole population. Obviously, further empirical studies are needed in order to pursue this further.

Understanding what factors generate the deduced seasonal density-dependent structures remains a challenge, requiring in-depth experimental work. Care is certainly required when interpreting statistical results of this kind. Indeed, based on results reported by Kaitala & Ranta (2001) and Jonzén *et al.* (2002), the deduced statistical lag-model(s) may be due to both density-dependent processes (which we have assumed) as well as density-*in*dependent processes (which we have ignored). However, irrespective of which interpretation we choose to adopt, the dynamic effect of changing season length (i.e. seasonal forcing) remains: the shorter the summer length becomes, the more likely it is that multi-annual cycles will occur.

We are indebted to the Forestry Agency of the Japanese Government for providing the data analysed in this paper. The study was partly supported by a grant-in-aid from the Ministry of Education, Science and Culture of Japan (no. 14340240). Furthermore, we acknowledge the support that we, over the years, have received from the Japan Society for the Promotion of Science, Forestry and Forest Products Research Institute of Japan, the Norwegian Research Council (NFR/NT), the Centre for Advanced Studies of the Norwegian Academy of Science and Letters, as well as the University of Oslo. Erik Bølviken is thanked for a series of most valuable discussions over the issues discussed in this paper. Kung-Sik Chan, Torbjørn Ergon, Rune Johansen, Tero Klemola, Ole Chr. Lingjærde, Atle Mysterud, Nigel G. Yoccoz and several anonymous reviewers provided valuable comments upon earlier versions of this paper. In particular, we thank two of the anonymous Proceedings B-reviewers for forcing us to further develop our argument: one for forcing us (essentially) to link the population dynamics and the season length more empirically (our fourth improvement), and another for forcing us to improve the basic re-parameterization over and beyond the Stenseth *et al.* formulation relying on a major simplifying assumption (our third improvement).

APPENDIX A: THE STATISTICAL OBSERVATION MODEL

The expected number of voles caught during a trapping session is related to the abundance of voles at the site and the trapping effort. Let the number of voles caught at a given site in year t to be given by z_t. The ecological annual process given by equation (3.1) is, as a first approximation, assumed to be linked to the observed number of voles caught through a Poisson model

$$P(z_t = z \mid x_t) = \exp(-\lambda_t)\lambda_t^z/z!, \qquad \text{(A 1)}$$

where the Poisson mean (assumed to be proportional to the trapping effort and the population abundance) is defined as

$$\lambda_t = qT_t\exp(\mu + x_t). \qquad \text{(A 2)}$$

The trapping effort T_t is a known quantity (see § 2) and x_t denotes the unknown log-abundance (centred around μ) for any year t. The parameter μ represents the mean of the log-transformed (true) population abundances. From the nature of the data, we cannot estimate the average level μ of the (true) population, nor the 'trappability' of the species in the given environment, q. However, we can estimate the product of the average level and the trappability, defined as $\exp(\gamma) = q\exp(\mu)$. This yields the following parameterization

$$\lambda_t = T_t\exp(\gamma + x_t). \qquad \text{(A 3)}$$

A graphical representation of the quantities in the annual model and their relationship is given in figure 3. (It is worth noticing that with this approach there is no need to add a constant in order to avoid taking logs of zeros (cf. Stenseth *et al.* 1996).)

A complete Bayesian model consists of the joint prior distribution for all unobservables (α_1, α_2, σ, λ, γ, and the log-abundance for each year t (x_1, x_2,…, x_N)) as well as the joint distribution of the observables (the abundance

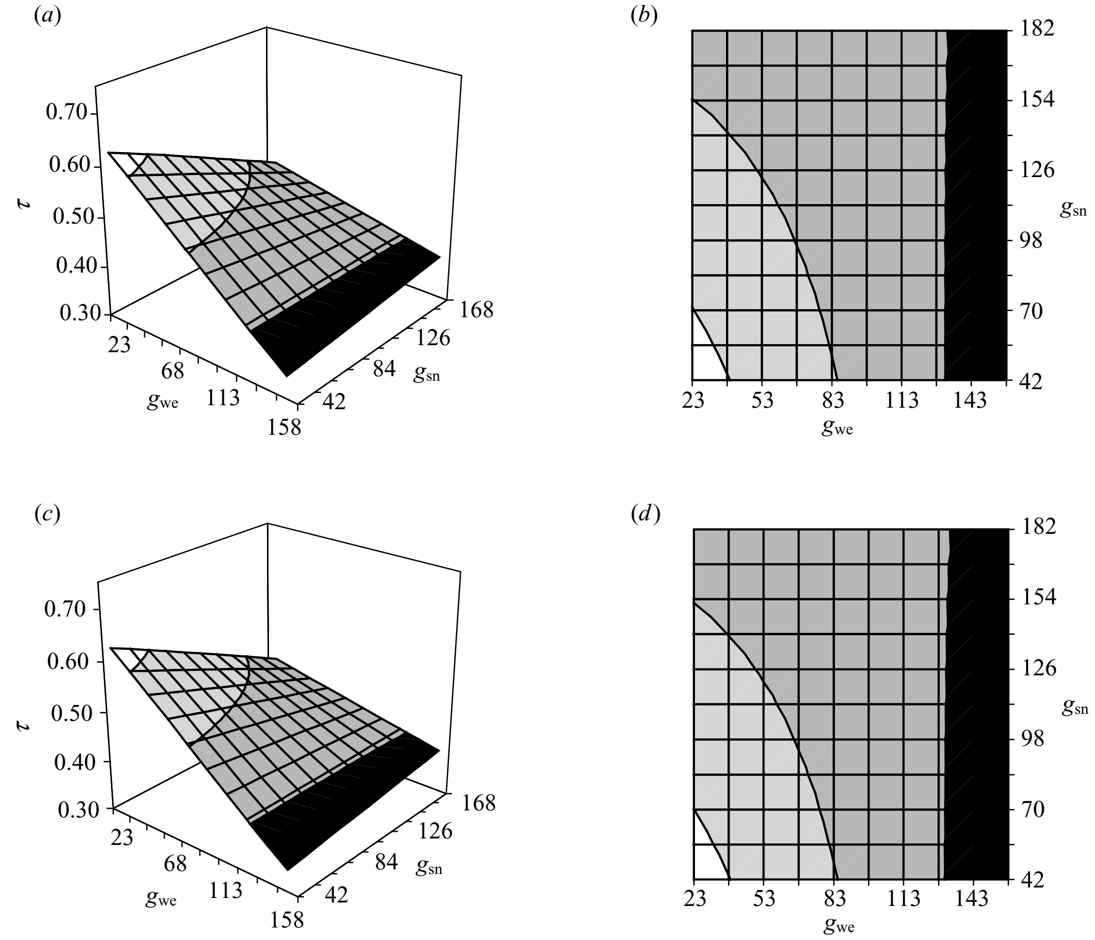

Figure 5. The values of τ as a function of geographical location (coordinates g_{we} and g_{sn}), as predicted from the optimum values of b_2 and b_3 (equations (3.6), (B 4) and (B 5)). (*a*) The predicted τ from the present analysis. The average of the two r^2 values was used as optimization criterion. (*b*) Same as (*a*), but shown as contour lines. (*c*) and (*d*) correspond to (*a*) and (*b*), but are obtained using the simplifying assumption that spring densities are mapped onto autumn densities (see electronic Appendix A). In the case of (*a*) and (*b*), equation (3.6) is given by $F = 0.998 - 0.011 - g_{we} - 0.0059 - g_{sn} + 4.5 \times 10^{-5} \times g_{we}g_{sn}$; in the case of (*c*) and (*d*), equation (3.6) is given by $F = 0.999 - 0.011 - g_{we} - 0.0060 - g_{sn} + 4.6 \times 10^{-5} \times g_{we}g_{sn}$.

data (z_1, z_2,..., z_N) and the trapping effort (T_1, T_2,..., T_N)). By conditioning on the data, the posterior distribution (i.e. the conditional probability of the unobservable quantities of interest, given the observed data) is calculated (by successive application of Bayes' theorem (e.g. Gelman *et al.* 1995)). The posterior distribution may usually not be obtained analytically but can be computed using Markov Chain Monte Carlo methods, like, for example, Gibbs sampling (Gilks *et al.* 1996). Bayesian inference is easily utilizable through the software package BUGS (Bayesian inference using Gibbs sampling (Spiegelhalter *et al.* 1999)). A Bayesian analysis (through the use of BUGS) is flexible and also easier to carry out than the more classical approach of using maximum-likelihood estimation (Meyer & Millar 1999*a*,*b*; Tufto *et al.* 2000).

To fully specify our model, a prior distribution has to be defined for all parameters that are not directly conditioned on other quantity or observed data (i.e. nodes in the graph without any 'parents'; α_1, α_2, σ and γ). Only vague (i.e. essentially flat) prior distributions were used ($\alpha_1 \sim N(0,100)$, $\alpha_2 \sim N(0,100)$, $\gamma \sim N(0,100)$ and $1/\sigma^2 \sim$ gamma distribution (0.001, 0.001)), meaning that the prior assumes essentially nothing about the parameters relative to what is learned from the sample. We performed 90 000 iterations of the Gibbs sampler, using WINBUGS (the BUGS version for Windows; http://www.mrc-bsu.cam.ac.uk/bugs/) v. 1.2, after a 'burn-in' of 10 000 iterations. (Using a few arbitrary selected series, preliminary analyses (applying the extensive convergence statistics available in the CODA software of Best *et al.* (1995)) suggested that the 'burn-in' period and the sample size were appropriate.) Convergence was assessed through the runs of multiple chains, and for each run comparing estimates from the first and second half of the chains. Moreover, autocorrelations within the chains seemed to be reasonably low (indicating that the mixing of the Gibbs sampler is not too slow; e.g. Raftery & Lewis 1992). Posterior means of α_1 and α_2 were taken as the estimates of annual direct and delayed density dependencies (see electronic Appendix A, table 3) and utilized in further analyses (using a frequentist approach).

APPENDIX B: DETERMINING THE PARAMETERS OF EQUATION (3.6)

We assume that τ, the length of the breeding season, is a logistic function of the geographical location:

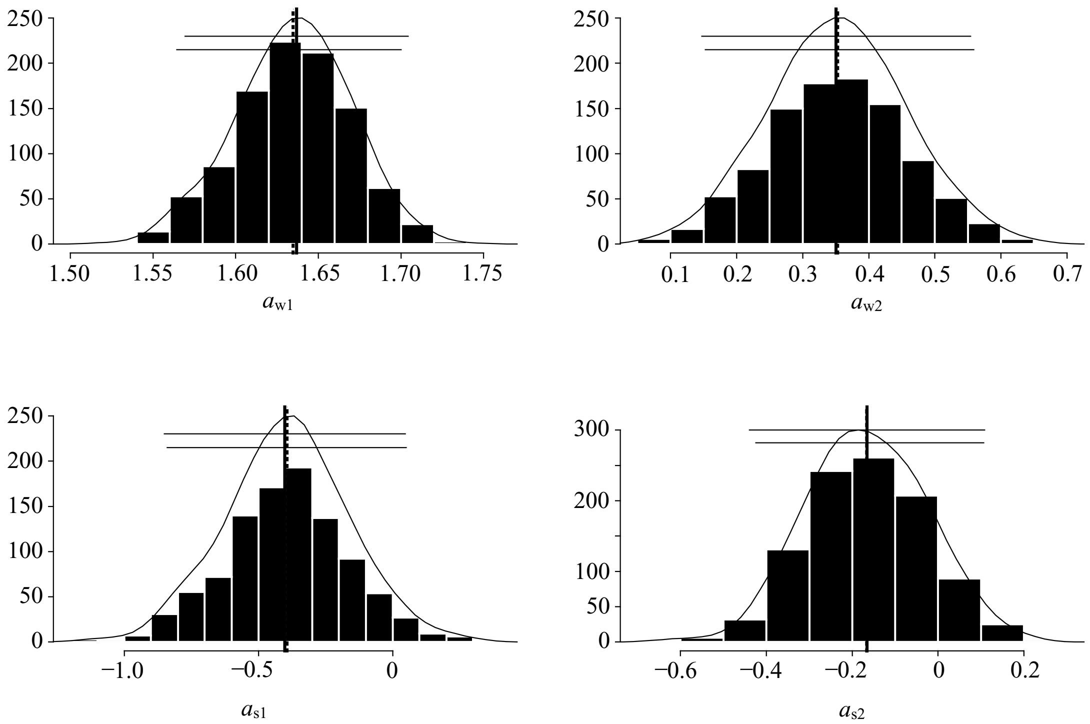

Figure 6. Estimates of $a_{\mathrm{s}1}$, $a_{\mathrm{s}2}$, $a_{\mathrm{w}1}$ and $a_{\mathrm{w}2}$ based on 1000 bootstrap analyses of α_1, α_2 and τ, where τ was computed from the chosen b_2–b_3 combination. Each panel shows a histogram and a probability density curve of the estimated values, as well as the estimated value based on all data (vertical unbroken line), the average of the bootstrapped estimates (vertical broken line), a CI based on the estimated value ± 1.96 times the s.d. of the bootstrapped values (upper horizontal line) and a CI based on the 2.5 and 97.5 percentiles of the bootstrapped values (upper horizontal line).

$$\tau_i = \frac{8.5}{12} = \frac{\exp(f(g_{\mathrm{we},i}, g_{\mathrm{sn},i}))}{1 + \exp(f(g_{\mathrm{we},i}, g_{\mathrm{sn},i}))}, \qquad \text{(B 1)}$$

where $f(g_{\mathrm{we},1}, g_{\mathrm{sn},1}) = b_0 + b_1 g_{\mathrm{we},1} + b_2 g_{\mathrm{sn},1} + b_3 g_{\mathrm{we},1} g_{\mathrm{sn},1}$.

To determine b_0, b_1, b_2 and b_3 of equation (B 1), we start by assuming that τ, the length of the breeding season, is $\tau_1 = 8.5$ months in the southwest ($g_{\mathrm{we},1} = 4.3$, $g_{\mathrm{sn},1} = 11.3$) and $\tau_2 = 4.5$ months in the northeast ($g_{\mathrm{we},2} = 157.87$, $g_{\mathrm{sn},2} = 146.54$) (e.g. Kaneko *et al.* 1998). Neither the locations of the geographical reference points nor the assumed season length at these points are critical assumptions; they are merely chosen to achieve an easier interpretation of the results in biological terms. These assumptions are expressed as

$$b_0 + b_1 g_{\mathrm{we},1} + b_2 g_{\mathrm{sn},1} + b_3 g_{\mathrm{we},1} g_{\mathrm{sn},1} = \ln\left(\frac{\tau_1}{1 - \tau_1}\right) = \mathrm{logit}(\tau_1) = 0.8873, \qquad \text{(B 2)}$$

$$b_0 + b_1 g_{\mathrm{we},2} + b_2 g_{\mathrm{sn},2} + b_3 g_{\mathrm{we},2} g_{\mathrm{sn},2} = \ln\left(\frac{\tau_2}{1 - \tau_2}\right) = \mathrm{logit}(\tau_2) = -0.5108. \qquad \text{(B 3)}$$

After some algebra, we can express b_1 in terms of b_2 and b_3, and b_0 in terms of b_1, b_2 and b_3:

$$b_1 = \frac{-0.5108 - 0.8873 + b_2(g_{\mathrm{sn},1} - g_{\mathrm{sn},2}) + b_3(g_{\mathrm{we},1} g_{\mathrm{sn},1} - g_{\mathrm{we},2} g_{\mathrm{sn},2})}{g_{\mathrm{we},2} - g_{\mathrm{we},1}}, \qquad \text{(B 4)}$$

$$b_0 = 0.8873 - b_1 g_{\mathrm{we},1} - b_2 g_{\mathrm{sn},1} - b_3 g_{\mathrm{we},1} g_{\mathrm{sn},1}. \qquad \text{(B 5)}$$

We determined b_0, b_1, b_2 and b_3 by searching through a large number of b_2–b_3 combinations. For each combination, we computed b_0 and b_1, then computed τ for each location, after which we used nonlinear regression to determine the values of the parameters $a_{\mathrm{s}1}$, $a_{\mathrm{s}2}$, $a_{\mathrm{w}1}$ and $a_{\mathrm{w}2}$ providing the best fit of equations (3.3) and (3.4) to the data. Finally, we chose the $b_2 - b_3$ combination with the highest average r^2-value. We estimated the standard errors and confidence intervals (CIs) of $a_{\mathrm{s}1}$, $a_{\mathrm{s}2}$, $a_{\mathrm{w}1}$ and $a_{\mathrm{w}2}$ based on 1000 bootstrap samples of α_1, α_2 and τ, where τ was computed from the chosen optimal b_2–b_3 combination.

The optimization with respect to b_2 and b_3, jointly with finding the parameters $a_{\mathrm{s}1}$, $a_{\mathrm{s}2}$, $a_{\mathrm{w}1}$ and $a_{\mathrm{w}2}$ by nonlinear regression, is depicted in figure 4, and the resulting τ-function across the geographical space of Hokkaido is depicted in figure 5. The distributions of the bootstrapped estimates of $a_{\mathrm{s}1}$, $a_{\mathrm{s}2}$, $a_{\mathrm{w}1}$ and $a_{\mathrm{w}2}$ are shown in figure 6.

We have confirmed (results not shown) that the same geographical pattern as found in this paper arises if the original index of Stenseth *et al.* (1998), as well as modifications thereof, are used.

REFERENCES

Åström, M., Lundberg, P. & Lundberg, S. 1996 Population dynamics with sequential density dependencies. *Oikos* **75**, 174–181.

Best, N. G., Cowles, M. K. & Vines, S. K. 1995 *Coda convergence diagnosis and output analysis software for Gibbs sampler output: v. 0.3.* Cambridge: MRC Biostatistics Unit, Institute of Public Health.

Bjørnstad, O. N., Falck, W. & Stenseth, N. C. 1995 A geographic gradient in small rodent density fluctuations: a statistical modelling approach. *Proc. R. Soc. Lond.* B **262**, 127–133.

Bjørnstad, O. N., Champley, S., Stenseth, N. C. & Saitoh, T.

1996 Cyclicity and stability of grey-sided voles, *Clethrionomys rufocanus*, of Hokkaido: evidence from spectral and principal component analysis. *Phil. Trans. R. Soc. Lond.* B **351**, 867–875.

Bjørnstad, O. N., Stenseth, N. C., Saitoh, T. & Lingjærde, O. C. 1998 Mapping the regional transition to cyclicity in *Clethrionomys rufocanus*: spectral densities and functional data analysis. *Res. Popul. Ecol.* **40**, 77–84.

Bjørnstad, O. N., Saitoh, T. & Stenseth, N. C. 1999 Synchrony and scaling in dynamics of voles and mice in northern Japan. *Ecology* **80**, 622–637.

Burnham, K. P. & Anderson, D. R. 1998 *Model selection and inference: a practical information–theoretic approach*. New York: Springer.

de Valpine, P. & Hastings, A. 2002 Fitting population models incorporating process noise and observation error. *Ecol. Monogr.* **72**, 57–76.

Fahrmeir, L. & Tutz, G. 1994 *Multivariate statistical modelling based on generalized linear models*. New York: Springer.

Gelman, A., Carlin, J. B., Stern, H. S. & Rubin, D. B. 1995 *Bayesian data analysis*. London: Chapman & Hall.

Gilks, W. R., Richardson, S. & Spiegelhalter, D. J. 1996 *Markov chain Monte Carlo in practice*. London: Chapman & Hall.

Grenfell, B. T. & Finkenstädt, B. F. 1998 Seasonality, stochasticity and population cycles. *Res. Popul. Ecol.* **40**, 141–143.

Hansen, T. F., Stenseth, N. C. & Henttonen, H. 1999 Multiannual vole cycles and population regulation during long winters: an analysis of seasonal density dependence. *Am. Nat.* **154**, 129–139.

Hanski, I., Hansson, L. & Henttonen, H. 1991 Specialist predators, generalist predators, and the microtine rodent cycle. *J. Anim. Ecol.* **60**, 353–367.

Hansson, L. 1971 Habitat, food and population dynamics of the field vole *Microtus agrestis* (L.) in southern Sweden. *Viltrevy* **8**, 267–378.

Hansson, L. 1987 An interpretation of rodent dynamics as due to trophic interactions. *Oikos* **50**, 308–318.

Hansson, L. & Henttonen, H. 1985 Gradients in density variations of small rodents: the importance of latitude snow cover. *Oecologia* **67**, 394–402.

Hansson, L. & Henttonen, H. 1988 Rodent dynamics as community processes. *Trends Ecol. Evol.* **3**, 195–200.

Hansson, L. & Henttonen, H. 1998 Rodent fluctuations in relation to seasonality in Fennoscandia and Hokkaido. *Res. Popul. Ecol.* **40**, 127–129.

Henttonen, H., Hansson, L. & Saitoh, T. 1992 Rodent dynamics and community structure: *Clethrionomys rufocanus* in northern Fennoscandia and Hokkaido. *Ann. Zool. Fenn.* **29**, 1–6.

Ims, R. 1990*a* The ecology and evolution of reproductive synchrony. *Trends. Ecol. Evol.* **5**, 135–140.

Ims, R. 1990*b* On the adaptive value of reproductive synchrony as a predator-swamping strategy. *Am. Nat.* **136**, 485–498.

Jedrzejewski, W. & Jedrzejewska, B. 1996 Rodent cycles in relation to biomass and productivity of ground vegetation and predation in the palearctic. *Acta Theriol.* **41**, 1–34.

Jonzén, N., Lundberg, P., Ranta, E. & Kaitala, V. 2002 The irreducible uncertainty of the demography–environment interaction in ecology. *Proc. R. Soc. Lond.* B **269**, 221–225. (DOI 10.1098/rspb.2001.1888.)

Kaitala, V. & Ranta, E. 2001 Is the impact of environmental noise visible in the dynamics of age-structured populations? *Proc. R. Soc. Lond.* B **268**, 1769–1774. (DOI 10.1098/rspb.2001.1718.)

Kaneko, Y., Nakata, K., Saitoh, T., Stenseth, N. C. & Bjørnstad, O. N. 1998 The biology of the vole *Clethrionomys rufocanus*: a review. *Res. Popul. Ecol.* **40**, 21–37.

Kira, T. 1949 Fundamental problems of climate classification. *Seibutsu Kagaku* **1**, 193–199.

Kira, T. 1971 *Nature from the ecological view point*. Tokyo: Kawaide-shobo.

Kleinbaum, D. G., Kupper, L. L. & Muller, K. E. 1988 *Applied regression analysis and other multivariable methods*. Belmont, CA: Duxbury Press.

Korpimäki, E., Norrdahl, K., Klemola, T., Pettersen, T. & Stenseth, N. C. 2002 Dynamic effects of predators on cyclic voles: field experimentation and model extrapolation. *Proc. R. Soc. Lond.* B **269**, 991–997. (DOI 10.1098/rspb.2002.1972.)

Kot, M. & Schaffer, W. M. 1984 The effects of seasonality on discrete models of population growth. *Theor. Popul. Biol.* **26**, 340–360.

Lindström, J., Ranta, E., Kokko, H., Lundberg, P. & Kaitala, V. 2001 From arctic lemmings to adaptive dynamics: Charles Elton's legacy in population ecology. *Biol. Rev.* **76**, 129–158.

Ludwig, D. & Walters, C. J. 1981 Measurement errors and uncertainty in parameter estimates for stock and recruitment. *Can. J. Fish. Aquat. Sci.* **38**, 711–720.

Merritt, J. F., Lima, M. & Bozinovic, F. 2001 Seasonal regulation in fluctuating small mammal populations: feedback structure and climate. *Oikos* **94**, 505–514.

Meyer, R. & Millar, R. B. 1999*a* Bayesian stock assessment using a state-space implementation of the delay difference model. *Can. J. Fish. Aquat. Sci.* **56**, 37–52.

Meyer, R. & Millar, R. B. 1999*b* BUGS in Bayesian stock assessments. *Can. J. Fish. Aquat. Sci.* **56**, 1078–1086.

Ota, K. 1958 Studies on the interspecific relationship of murid rodents. III. Habitat segregation in a small tree stand. *Jpn J. Ecol.* **8**, 149–156.

Ota, K. 1984 *Study on wild murid rodents in Hokkaido*. Sapporo, Japan: Hokkaido University Press.

Raftery, A. L. & Lewis, S. 1992 How many iterations in the Gibbs sampler? In *Bayesian statistics*, vol. 4 (ed. J. M. Bernardo, J. O. Berger, A. P. Dawid & A. F. M. Smith), pp. 763–774. Oxford University Press.

Reddingius, J. & den Boer, P. J. 1989 On the stabilization of animal numbers. Problems of testing. 1. Power estimates and estimation errors. *Oecologia* **78**, 1–8.

Rinaldi, S., Muratori, S. & Kuznetsov, Y. 1993 Multiple attractors, catastrophes and chaos in seasonally perturbed predator–prey communities. *J. Math. Biol.* **55**, 15–35.

Rothery, P. 1998 The problems associated with the identification of density dependence in population data. In *Insect populations* (ed. J. P. Dempster & I. F. G. McLean), pp. 97–133. Dordrecht, The Netherlands: Kluwer.

Royama, T. 1992 *Analytical population dynamics*. London: Chapman & Hall.

Saitoh, T. 1987 A time series and geographical analysis of population dynamics of the red-backed vole in Hokkaido, Japan. *Oecologia* **73**, 382–388.

Saitoh, T. & Nakatsu, A. 1997 Impact of forest plantation on the community of small mammals in Hokkaido, Japan. *Mammal Study* **22**, 27–38.

Saitoh, T., Stenseth, N. C. & Bjørnstad, O. N. 1997 Density-dependence in fluctuating grey-sided vole populations. *J. Anim. Ecol.* **66**, 14–24.

Saitoh, T., Stenseth, N. C. & Bjørnstad, O. N. 1998 The population dynamics of the vole *Clethrionomys rufocanus* in Hokkaido, Japan. *Res. Popul. Ecol.* **40**, 61–76.

Saitoh, T., Bjørnstad, O. N. & Stenseth, N. C. 1999 Density dependence in voles and mice: a comparative study. *Ecology* **80**, 638–650.

Saitoh, T., Stenseth, N. C., Viljugrein, H. & Kittilsen, K. O. 2002 Seasonal processes in density dependence of fluctuating vole populations. *Popul. Ecol.* (Submitted.)

Shenk, T. M., White, G. C. & Burnham, K. P. 1998 Sampling-variance effects on detecting density dependence from temporal trends in natural populations. *Ecol. Monogr.* **68**, 445–463.

Spiegelhalter, D. J., Thomas, A. & Best, N. G. 1999 *WinBugs v. 1.2 user manual*. Cambridge: MRC Biostatistics Unit, Institute of Public Health.

Stenseth, N. C. 1999 Population cycles in voles and lemmings: density dependence and phase dependence in a stochastic world. *Oikos* **87**, 427–461.

Stenseth, N. C., Bjørnstad, O. N. & Saitoh, T. 1996 A gradient from stable to cyclic populations of *Clethrionomys rufocanus* in Hokkaido, Japan. *Proc. R. Soc. Lond.* B **263**, 1117–1126.

Stenseth, N. C., Bjørnstad, O. N. & Saitoh, T. 1998 Seasonal forcing on the dynamics of *Clethrionomys rufocanus*: modelling geographic gradients in population dynamics. *Res. Popul. Ecol.* **40**, 85–95.

Stenseth, N. C., Viljugrein, H., Jedrzejewski, W., Mysterud, A. & Pucek, Z. 2002 Population dynamics of *Clethrionomys glarolus* and *Apodemus flavicolus*: seasonal components of density-dependence and density-independence. *Acta Theriol.* **47**(Suppl.), 36–67.

Tatewaki, M. 1958 Forest ecology of the islands of the north Pacific ocean. *J. Faculty Agriculture Hokkaido Univ.* **50**, 371–472.

Tufto, J., Saether, B.-E., Engen, S., Arcese, P., Jerstad, K., Røstad, O. W. & Smith, J. N. M. 2000 Bayesian meta-analysis of demographic parameters in three small temperate passerines. *Oikos* **88**, 273–281.

Turchin, P. & Hanski, I. 1997 An empirically based model for latitudinal gradient in vole population dynamics. *Am. Nat.* **149**, 842–874.

Ueda, M., Higuchi, S., Igarashi, B., Maeda, M., Kuwahata, T., Ota, K., Abe, H., Fujimaki, Y., Fujikura, J. & Takayasu, T. 1966 Historical review of studies on the Bedford's red-backed vole, *Clethrionomys rufocanus bedfordiae* (Thomas). *Bull. Govmnt Forest Exp. Station* (*Tokyo*) **191**, 1–100.

As this paper exceeds the maximum length normally permitted, the authors have agreed to contribute to production costs.

Visit http://www.pubs.royalsoc.ac.uk to see an electronic appendix to this paper.